

Report | HW3

CS754 - Advanced Image Processing

Omkar Shirpure (22B0910)
Krish Rakholiya (22B0927)
Suryansh Patidar (22B1036)



Contents

1	Q1	1
2	Q2	6
3	Q3	14
4	Q4	16
5	Q5	18

Declaration: The work submitted is our own, and we have adhered to the principles of academic honesty while completing and submitting this work. We have not referred to any unauthorized sources, and we have not used generative AI tools for the work submitted here.

1 Q1

(a)

Theorem 3 (from Class Notes)

Consider a matrix $A = \Phi\Psi$ of size $m \times n$, where:

- Φ is the sensing matrix ($m \times n$),
- Ψ is the basis matrix ($n \times n$),
- The Restricted Isometry Property (RIP) holds for order $2S$ with $\delta_{2S} < 0.41$.

Given a measurement vector $y = \Phi\Psi\theta + \eta$, where η is noise, we solve:

$$\min \|\theta\|_1 \quad \text{such that} \quad \|y - \Phi\Psi\theta\|_2^2 \leq \epsilon. \quad (1)$$

The solution θ^* satisfies:

$$\|\theta^* - \theta\|_2 \leq \frac{C_0}{\sqrt{S}} \|\theta - \theta_S\|_1 + C_1 \epsilon, \quad (2)$$

where θ_S is obtained by retaining the top S largest magnitude elements of θ .

Theorem 11.1 from Statistical Learning with Sparsity

The LASSO estimator minimizes:

$$J(\beta) = \frac{1}{2N} \|y - X\beta\|_2^2 + \lambda_N \|\beta\|_1, \quad (3)$$

where:

- X is a sensing matrix ($N \times p$) with unit-normalized columns,
- $y = X\beta + w$ is the measurement vector,
- $w \sim \mathcal{N}(0, \sigma^2 I)$ is Gaussian noise,
- λ_N is a regularization parameter.

The error bound for LASSO:

$$\|\hat{\beta} - \beta^*\|_2 \leq \frac{c\sigma}{\sqrt{\gamma}} \sqrt{\frac{k \log p}{N}}, \quad (4)$$

which holds with high probability. For compressible signals:

$$\|\hat{\beta} - \beta^*\|_2 \leq c\sigma \sqrt{\frac{k \log(ep/k)}{N}}. \quad (5)$$

The required sample size:

$$N \geq k \log(ep/k). \quad (6)$$

Comparison of Error Bounds

- **Number of Measurements (N):**
 - **LASSO:** Error scales as $O\left(\sqrt{\frac{k \log p}{N}}\right)$, meaning more measurements reduce the error.
 - **Theorem 3:** Error has a term $\frac{1}{\sqrt{S}}\|\theta - \theta_S\|_1$, indicating that more measurements (improving sparsity reconstruction) lower the error.
- **Signal Sparsity (k or S):**
 - **LASSO:** Error is proportional to \sqrt{k} , meaning sparser signals (smaller k) result in lower error.
 - **Theorem 3:** Includes $\|\theta - \theta_S\|_1$, meaning better approximability with S -sparsity leads to lower error.
- **Noise Standard Deviation (σ):**
 - **LASSO:** Error scales as $O(\sigma)$.
 - **Theorem 3:** Includes $C_1\epsilon$, where ϵ depends on noise power.
- **Signal Dimension (p or n):**
 - **LASSO:** The bound includes a logarithmic dependence on p , making it effective for high-dimensional settings.
 - **Theorem 3:** Does not explicitly include n or p , but they implicitly affect the RIP condition.

Intuition and Interpretability

- **Theorem 3** is more intuitive in terms of sparsity reconstruction and provides an explicit connection to compressed sensing theory.
- **LASSO bounds** are more statistical, relying on high-probability guarantees and asymptotics.
- For a practical setting, **Theorem 3 is more interpretable** for understanding reconstruction in compressed sensing, whereas **LASSO bounds are stronger for statistical estimation in general settings**.

Conclusion

- If focusing on **sparse signal reconstruction**, Theorem 3 is more useful due to its direct relation to RIP and approximation error.
- If considering a **broader statistical learning context**, the LASSO bounds provide a more general and rigorous error estimate.

(b)

Strong Convexity: Given a differentiable function $f : \mathbb{R}^p \rightarrow \mathbb{R}$, Strong convexity at a point $\beta \in \mathbb{R}^p$ is defined as

$$f(\beta') - f(\beta) \geq \nabla f(\beta)^\top (\beta' - \beta) + \frac{\gamma}{2}\|\beta' - \beta\|_2^2 \quad \forall \beta' \in \mathbb{R}^p$$

where $\gamma > 0$. Strong convexity allows us to state that if $|f(\beta') - f(\beta)|$ is small, $\|\beta' - \beta\|_2$ is even smaller. Now we try to find conditions for the least-squares objective function:

$$f_N(\beta) = \frac{1}{2N}\|y - X\beta\|_2^2$$

to be strongly convex. For that, the double derivative matrix wrt β

$$\nabla^2 f(\beta) = X^T X / N$$

should have all its eigenvalues uniformly bounded away from zero. However, the rank of the matrix $X^T X$ can be at most $\min\{N, p\}$, as $X \in R^{p \times N}$. Thus, it's always rank deficient and hence, not strongly convex when $N < p$. Thus we need to relax our notion of strong convexity and we define the restricted strong convexity condition:

A function f satisfies restricted strong convexity at β^* with respect to $C \subset R^p$ if there is a constant $\gamma > 0$ st:

$$\frac{v^T \nabla^2 f(\beta)v}{\|v\|_2^2} \geq \gamma$$

for all nonzero $v \in C$, and for all $\beta \in R^p$ in a neighborhood of β^* . Thus, in our case (restricted eigenvalues)

$$\frac{\frac{1}{N} v^T X^T X v}{\|v\|_2^2} \geq \gamma \quad (7)$$

for all nonzero $v \in C$. Therefore, the minimum value of LHS, which is the minimum eigenvalue λ_{\min} should be greater than γ

$$\lambda_{\min} \geq \gamma, \quad \forall v \in C, v \neq 0$$

This is the restricted eigenvalue condition

(c)

Lagrangian Lasso:

$$G(v) = \frac{1}{2N} \|y - X(\beta^* + v)\|_2^2 + \lambda_N \|\beta^* + v\|_1$$

Its given that $\hat{v} = \hat{\beta} - \beta^*$, minimizes G by construction, hence we have

$$G(\hat{v}) \leq G(0) \quad (8)$$

(d)

$$\frac{1}{2N} \|y - X(\beta^* + \hat{v})\|_2^2 + \lambda_N \|\beta^* + \hat{v}\|_1 \leq \frac{1}{2N} \|y - X(\beta^*)\|_2^2 + \lambda_N \|\beta^*\|_1$$

Now since $y = X\beta^* + w$, implying $w = y - X\beta^*$, we get

$$\frac{1}{2N} \|w - X\hat{v}\|_2^2 - \frac{1}{2N} \|w\|_2^2 \leq \lambda_N \|\beta^*\|_1 - \lambda_N \|\beta^* + \hat{v}\|_1$$

Expanding:

$$\begin{aligned} \frac{1}{2N} (w - X\hat{v})^T (w - X\hat{v}) - \frac{1}{2N} w^T w &\leq \lambda_N (\|\beta^*\|_1 - \|\beta^* + \hat{v}\|_1) \\ \implies \frac{\hat{v}^T X^T X \hat{v}}{2N} - \frac{w^T X \hat{v}}{N} &\leq \lambda_N (\|\beta^*\|_1 - \|\beta^* + \hat{v}\|_1) \end{aligned}$$

Rewriting,

$$\frac{\|X\hat{v}\|_2^2}{2N} \leq \frac{w^T X \hat{v}}{N} + \lambda_N (\|\beta^*\|_1 - \|\beta^* + \hat{v}\|_1) \quad (9)$$

(e)

Consider the Lagrangian lasso with a regularization parameter $\lambda_N \geq \frac{2}{N} \|X^T w\|_\infty$. We will prove the two bounds stated in Theorem 11.2.

Proof of Bound (11.25a)

We begin with equation 11.21 from above:

$$\begin{aligned} 0 &\leq \frac{w^T X \hat{v}}{N} + \lambda_N (\|\beta^*\|_1 - \|\beta^* + \hat{\nu}\|_1) \\ 0 &\leq \frac{\|X^T w\|_\infty}{N} \|\hat{\nu}\|_1 + \lambda_N (\|\beta^*\|_1 - \|\beta^* + \hat{\nu}\|_1) \end{aligned}$$

Using the assumption $\frac{\|X^T w\|_\infty}{N} \leq \frac{\lambda_N}{2}$, we obtain:

$$0 \leq \frac{\lambda_N}{2} \|\hat{\nu}\|_1 + \lambda_N (\|\beta^*\|_1 - \|\beta^* + \hat{\nu}\|_1)$$

Using triangle inequality:

$$\|\beta^* + \hat{\nu}\|_1 \geq \|\hat{\nu}\|_1 - \|\beta^*\|_1$$

Substituting, we get:

$$\begin{aligned} 0 &\leq \frac{\lambda_N}{2} \|\hat{\nu}\|_1 - \lambda_N \|\hat{\nu}\|_1 + 2\lambda_N \|\beta^*\|_1 \\ 0 &\leq \frac{\lambda_N}{2} (-\|\hat{\nu}\|_1 + 4R_1) \end{aligned}$$

Thus, $\|\hat{\nu}\|_1 \leq 4R_1$.

Going back to equation 11.21:

$$\begin{aligned} \frac{\|X \hat{v}\|_2^2}{2N} &\leq \frac{w^T X \hat{v}}{N} + \lambda_N (\|\beta^*\|_1 - \|\beta^* + \hat{\nu}\|_1) \\ \frac{\|X \hat{v}\|_2^2}{2N} &\leq \frac{\|X^T w\|_\infty}{N} \|\hat{\nu}\|_1 + \lambda_N (\|\beta^*\|_1 - \|\beta^* + \hat{\nu}\|_1) \end{aligned}$$

Proceeding in similar fashion as earlier,

$$\frac{\|X \hat{v}\|_2^2}{2N} \leq \frac{\lambda_N}{2} \|\hat{\nu}\|_1 + \lambda_N (\|\beta^*\|_1 - \|\beta^* + \hat{\nu}\|_1)$$

We use the triangle inequality again:

$$\|\beta^* + \hat{\nu}\|_1 \geq \|\beta^*\|_1 - \|\hat{\nu}\|_1$$

Substituting, we get:

$$\frac{\|X \hat{v}\|_2^2}{2N} \leq \frac{\lambda_N}{2} \|\hat{\nu}\|_1 + \lambda_N (\|\hat{\nu}\|_1) \leq 6\lambda_N R_1$$

which proves the first bound (11.25a).

Proof of Bound (11.25b)

We continue from the final equation in the earlier proof:

$$\frac{\|X \hat{v}\|_2^2}{N} \leq 3\lambda_N \|\hat{\nu}\|_1$$

We relate the L1 norm to L2 norm as follows:

$$\|\hat{\nu}\|_1 = \|\hat{\nu}_S\|_1 + \|\nu \hat{S}^c\|_1 \leq \|\hat{\nu}_S\|_1 \leq 2\sqrt{k} \|\hat{\nu}\|_2$$

Substituting, we get

$$\frac{\|X\hat{v}\|_2^2}{N} \leq 6\lambda_N\sqrt{k}\|\hat{v}\|_2 \leq 12\lambda_N\sqrt{k}\|\hat{v}\|_2$$

Lemma 11.1 states that if $\lambda_N \geq 2\|\frac{X^T W}{N}\|_\infty > 0$, the error $\hat{v} = \hat{\beta} - \beta^*$ associated with any Lasso solution $\hat{\beta}$ belongs to the cone set $C(S; 3)$. This allows us to apply the γ -RE condition to \hat{v} as shown:

$$\frac{\frac{1}{N}\nu X^T X\nu}{\|\nu\|_2} \geq \gamma$$

Applying this to \hat{v} :

$$\|\hat{v}\|_2^2 \leq \frac{1}{N\gamma} \|X\hat{v}\|_2^2$$

Substituting this, we obtain:

$$\begin{aligned} \frac{\|X\hat{v}\|_2^2}{N} &\leq 12\lambda_N\sqrt{k}\|\hat{v}\|_2 \\ \frac{\|X\hat{v}\|_2^4}{N^2} &\leq 144k\lambda_N^2\|\hat{v}\|_2^2 \leq 144k\lambda_N^2\left(\frac{1}{N\gamma}\|X\hat{v}\|_2^2\right) \\ \frac{\|X\hat{v}\|_2^2}{N} &\leq \frac{144}{\gamma}k\lambda_N^2 \end{aligned}$$

proving the second bound (11.25b).

This concludes the proof of Theorem 11.2.

2 Q2

Defining the variables

Let's first consider the equations for the patched case, then we can extend it to the direct case (single patch).

In the submitted code, the variable y defined at lines 47, 48 represents b in the equation $Ax = b$, which is a patch matrix taken from the coded exposure image E_u , and then reshaped into a column vector.

The variable A in the equation refers to the product $\text{phi} * \text{psi}$ in the code at lines 36, 41 – 45, 50, which is constructed as follows:

For patch (i, j) (i_{th} row, j_{th} column), let S_t be the t_{th} frame ($t = 1, 2, \dots, T$) from the i, j_{th} patch from C_t , and let $X(:)$ denote the vectorized version of X (reshaped into a column vector). Then

$$A = (\text{diag}(S_1(:)) \mid \text{diag}(S_2(:)) \mid \dots \mid \text{diag}(S_T(:)))$$

Now for the direct case, we can simply take the largest possible patch size (single patch), and use the same equations over patch $(1, 1)$.

Results

Cars - Frame 1



(a) CARS original frame=1



(b) CARS reconstructed frame=1,T=3



(a) CARS reconstructed frame=1,T=5



(b) CARS reconstructed frame=1,T=7

Cars - Frame 2



(a) CARS original frame=2



(b) CARS reconstructed frame=2,T=3



(a) CARS reconstructed frame=2,T=5



(b) CARS reconstructed frame=2,T=7

Cars - Frame 3

(a) CARS original frame=3



(b) CARS reconstructed frame=3,T=3



(a) CARS reconstructed frame=3,T=5



(b) CARS reconstructed frame=3,T=7

Cars - Frame 4

(a) CARS original frame=4



(a) CARS reconstructed frame=4,T=5



(b) CARS reconstructed frame=4,T=7

Cars - Frame 5



(a) CARS original frame=5



(a) CARS reconstructed frame=5,T=5



(b) CARS reconstructed frame=5,T=7

Cars - Frame 6

(a) CARS original frame=6



(b) CARS reconstructed frame=6,T=7

Cars - Frame 7

(a) CARS original frame=6



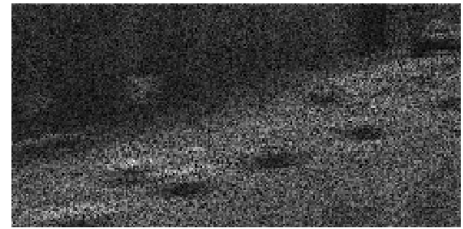
(b) CARS reconstructed frame=6,T=7

Cars - CODED

(a) CARS coded T=3



(a) CARS coded T=5



(b) CARS coded T=7

Cars - RMSE

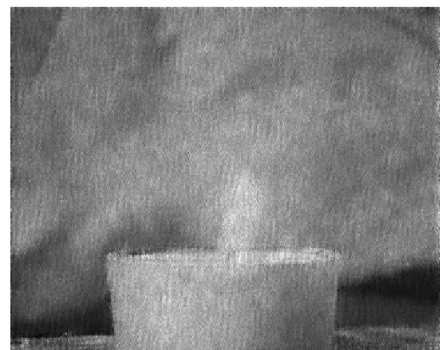
The calculated RMSE for the reconstructed subframes vs the original subframes are

- $T = 3, RMSE = 22.9026$
- $T = 5, RMSE = 29.7149$
- $T = 7, RMSE = 36.3463$

Flame - Frame 1



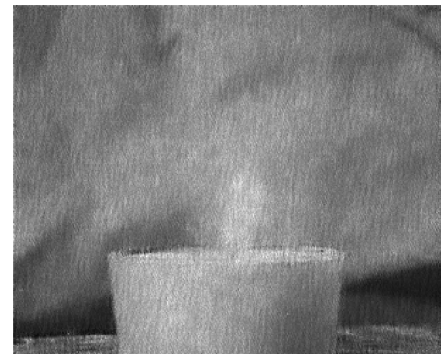
(a) FLAME original frame=1



(b) FLAME reconstructed frame=1,T=5

Flame - Frame 2

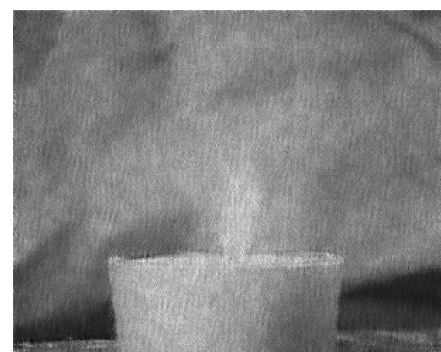
(a) FLAME original frame=2



(b) FLAME reconstructed frame=2,T=5

Flame - Frame 3

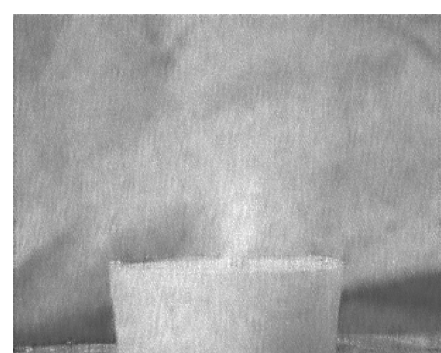
(a) FLAME original frame=3



(b) FLAME reconstructed frame=3,T=5

Flame - Frame 4

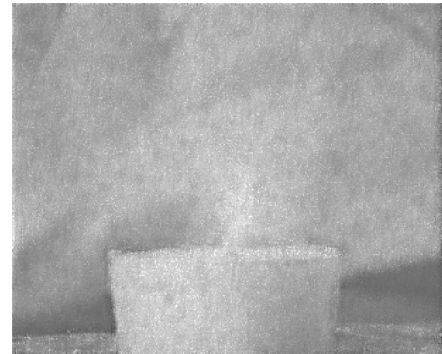
(a) FLAME original frame=4



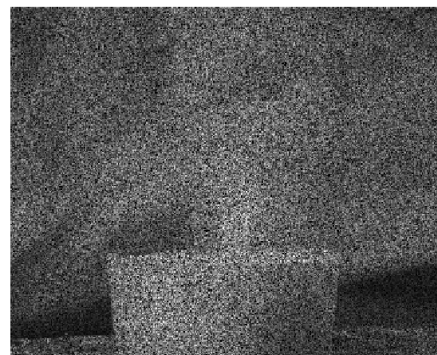
(b) FLAME reconstructed frame=4,T=5

Flame - Frame 5

(a) FLAME original frame=5



(b) FLAME reconstructed frame=5,T=5

Flame - CODED

(a) FLAME coded T=5

Flame - RMSE

The calculated RMSE for the reconstructed subframes vs the original subframes are

- $T = 5, RMSE = 26.0183$

3 Q3

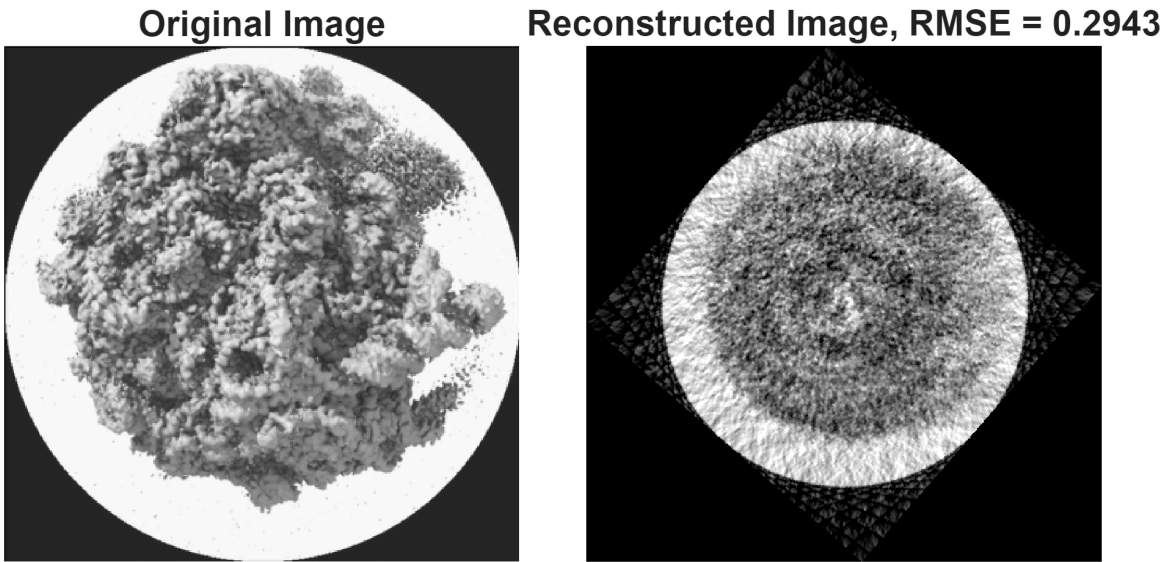


Figure 21: $N = 50$

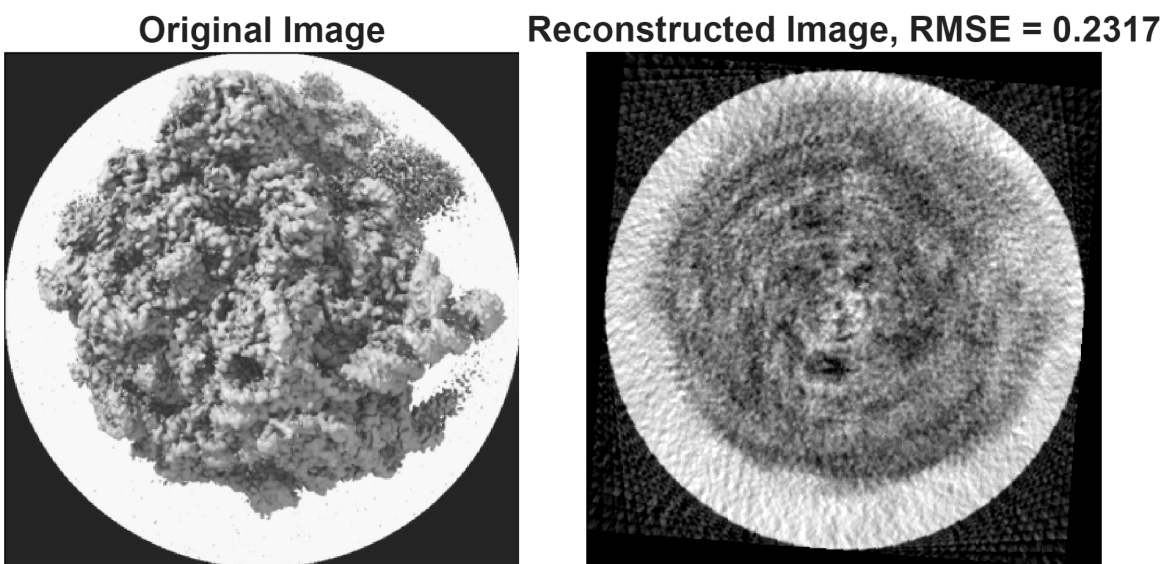


Figure 22: $N = 100$

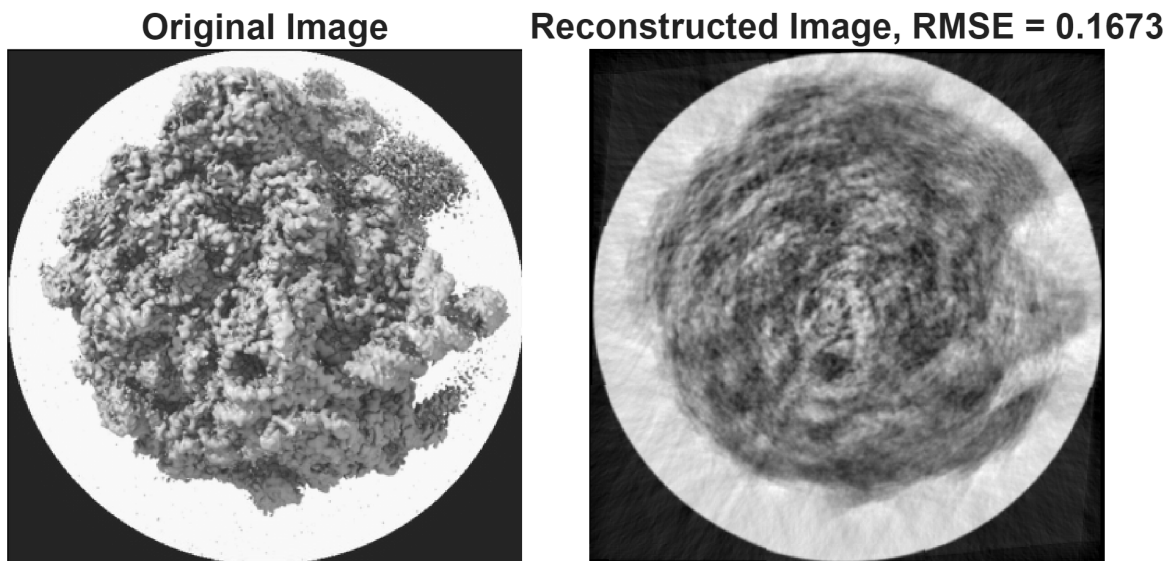


Figure 23: N = 500

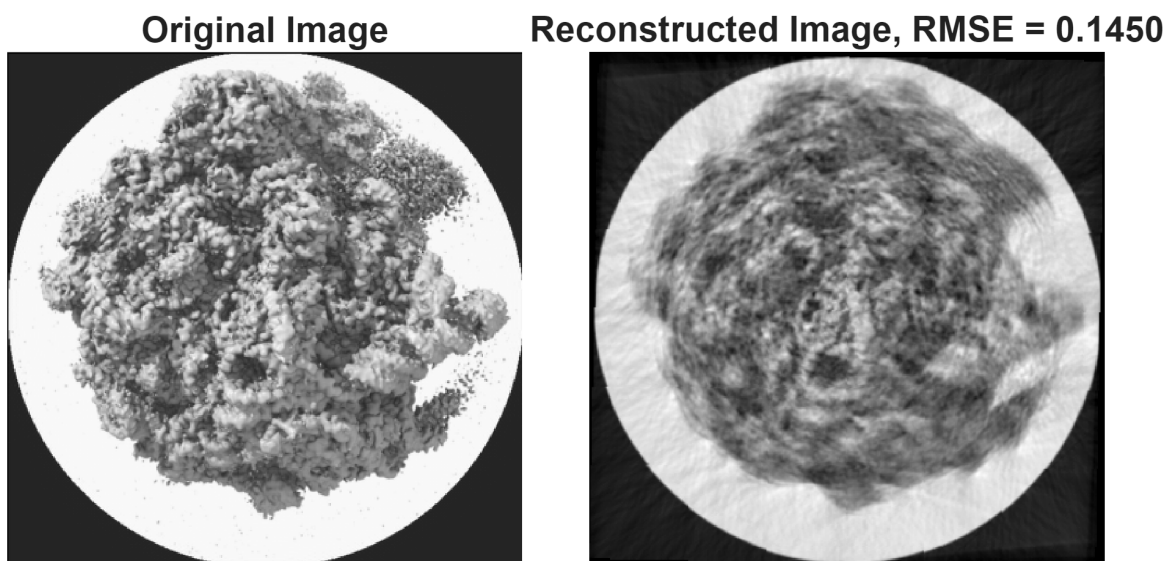


Figure 24: N = 1000

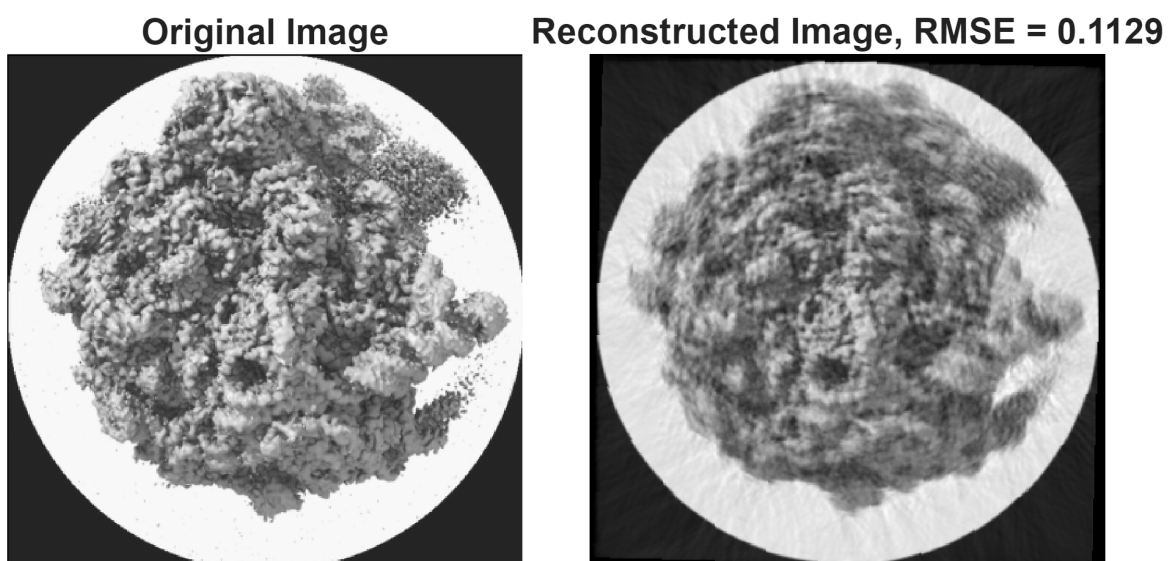


Figure 25: N = 2000

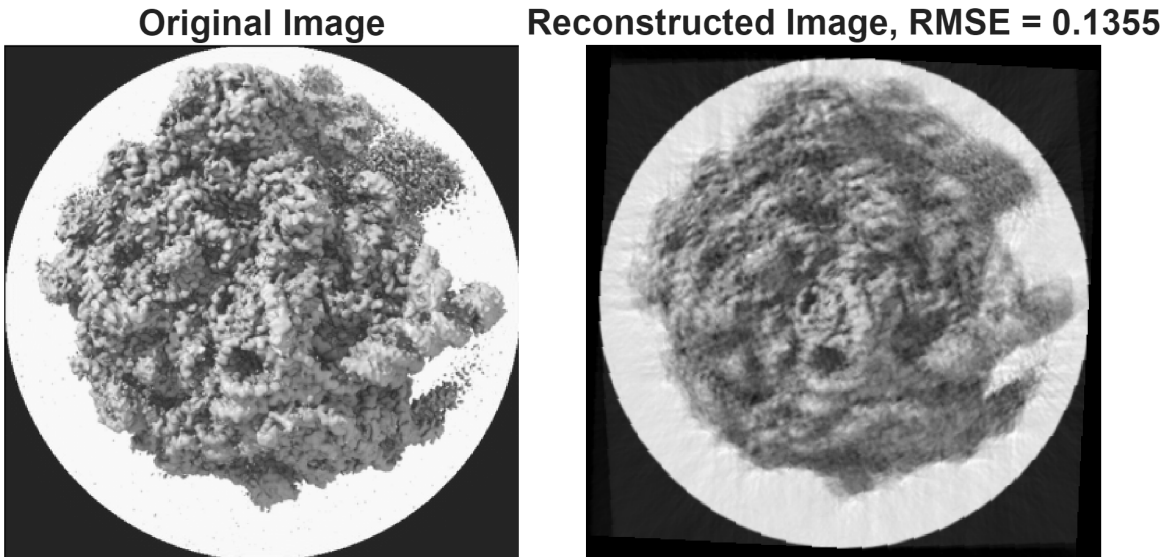


Figure 26: N = 5000

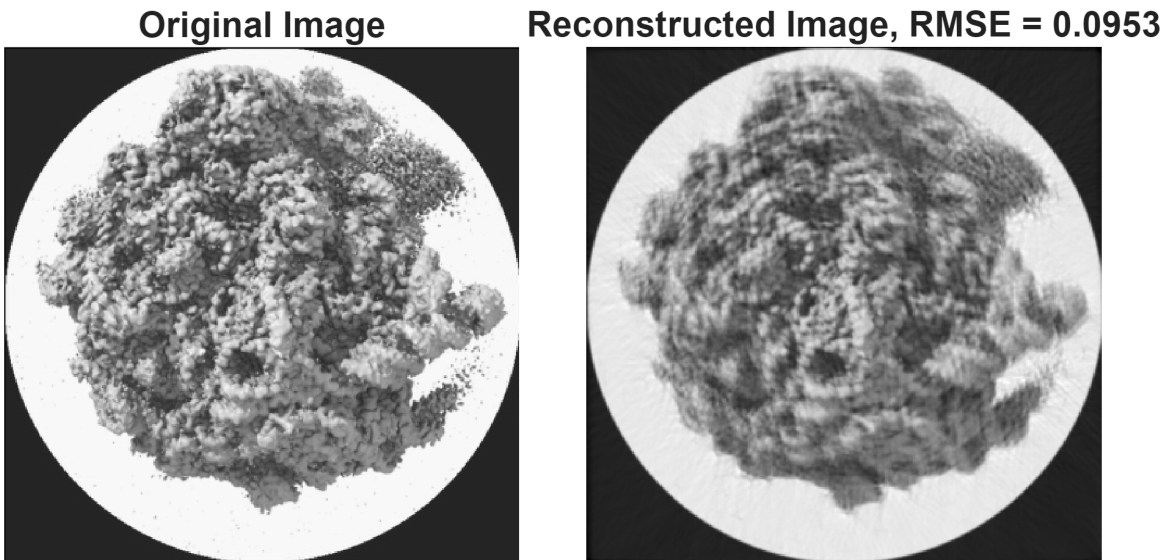


Figure 27: N = 10000

4 Q4

The Radon Transform of a 2-D image $f(x, y)$ at angle θ is defined as,

$$\mathcal{R}_\theta f(\rho) = \int_{-\infty}^{\infty} f(x, y) \delta(\rho - (x \cos \theta + y \sin \theta)) dx dy \quad (10)$$

Since $g(x, y)$ is another 2-D image which is a version of $f(x, y)$ shifted by (x_0, y_0) , we can write it as,

$$g(x, y) = f(x - x_0, y - y_0)$$

Further, the Radon Transform of $g(x, y)$ defined at angle θ can be written as

$$\begin{aligned}\mathcal{R}_\theta g(\rho) &= \int_{-\infty}^{\infty} g(x, y) \delta(\rho - (x \cos \theta + y \sin \theta)) dx dy \\ &= \int_{-\infty}^{\infty} f(x - x_0, y - y_0) \delta(\rho - (x \cos \theta + y \sin \theta)) dx dy\end{aligned}$$

Substitute $x' = x - x_0$ and $y' = y - y_0 \rightarrow$

$$\begin{aligned}&= \int_{-\infty}^{\infty} f(x', y') \delta(\rho - ((x' + x_0) \cos \theta + (y' + y_0) \sin \theta)) dx' dy' \\ &= \int_{-\infty}^{\infty} f(x', y') \delta((\rho - x_0 \cos(\theta) - y_0 \sin(\theta)) - (x' \cos \theta + y' \sin \theta)) dx' dy'\end{aligned}$$

Notice similarity with (1) \rightarrow

$$\begin{aligned}\mathcal{R}_\theta g(\rho) &= \mathcal{R}_\theta f(\rho - x_0 \cos(\theta) - y_0 \sin(\theta)) \\ \mathcal{R}_\theta g(\rho) &= \mathcal{R}_\theta f(\rho - \langle x_0, y_0 \rangle \cdot \langle \cos(\theta), \sin(\theta) \rangle)\end{aligned}$$

Hence proved!

5 Q5

Understanding the Problem

We have two particle images, Q_1 and Q_2 , which are 2D projections of a 3D density map. Each image is captured from a different 3D orientation and has undergone a 2D shift in the image plane.

- Q_1 is obtained by translating a zero-shift particle image P_1 by $(\delta x_1, \delta y_1)$.
- Q_2 is obtained by translating a zero-shift particle image P_2 by $(\delta x_2, \delta y_2)$.

Here, P_1 and P_2 are not directly observed; we only observe Q_1 and Q_2 .

- In P_1 , the common line passes through the origin at an angle θ_1 with respect to its X-axis.
- In P_2 , the common line passes through the origin at an angle θ_2 with respect to its X-axis.

The observed images Q_1 and Q_2 are shifted versions of P_1 and P_2 . Shifting an image translates all its features, including the common line.

- In Q_1 , the common line (originally at angle θ_1 in P_1) is now shifted by $(\delta x_1, \delta y_1)$.
- In Q_2 , the common line (originally at angle θ_2 in P_2) is now shifted by $(\delta x_2, \delta y_2)$.

The key observation is that the **common line in 3D space must correspond to the same physical feature in both projections**, even after the 2D shifts. This imposes a constraint relating the shifts and the common line angles.

Deriving the Relationship

The common line implies that the Fourier transforms of P_1 and P_2 share a central line (central slice theorem). The shifts $(\delta x, \delta y)$ introduce a linear phase ramp in the Fourier transform:

$$\begin{aligned}\mathcal{F}(Q_1) &= \mathcal{F}(P_1) \cdot e^{-2\pi i(u\delta x_1 + v\delta y_1)} \\ \mathcal{F}(Q_2) &= \mathcal{F}(P_2) \cdot e^{-2\pi i(u\delta x_2 + v\delta y_2)}\end{aligned}$$

On the common line in Fourier space (where $\mathcal{F}(P_1)$ and $\mathcal{F}(P_2)$ are equal), the phase difference must be consistent. This leads to:

$$e^{-2\pi i(u\delta x_1 + v\delta y_1)} = e^{-2\pi i(u\delta x_2 + v\delta y_2)}$$

for (u, v) along the common line direction. This implies:

$$u(\delta x_1 - \delta x_2) + v(\delta y_1 - \delta y_2) = n \quad (\text{for some integer } n)$$

Since this must hold for all (u, v) along the common line, the only solution is $n = 0$ and:

$$\begin{aligned}\delta x_1 - \delta x_2 &= -m \sin \theta \\ \delta y_1 - \delta y_2 &= m \cos \theta\end{aligned}$$

for some m , where θ is related to the common line angles. However, a more precise relationship can be derived by considering that the common line in Fourier space corresponds to a line at angle θ_1 in Q_1 and θ_2 in Q_2 . The phase difference along this line must vanish, leading to:

$$\delta x_1 \cos \theta_1 + \delta y_1 \sin \theta_1 = \delta x_2 \cos \theta_2 + \delta y_2 \sin \theta_2$$

This is the key equation relating the shifts and common line angles.

Determining the Shifts

Given the equation:

$$\delta x_1 \cos \theta_1 + \delta y_1 \sin \theta_1 = \delta x_2 \cos \theta_2 + \delta y_2 \sin \theta_2$$

We can use this to solve for the shifts:

1. For two images Q_1 and Q_2 , we can estimate θ_1 and θ_2 from the common line detection in Fourier space.
2. The equation provides one linear constraint on the four unknowns $\delta x_1, \delta y_1, \delta x_2, \delta y_2$.
3. To solve for the shifts, we need additional constraints.

Extending to N Images

For N images, we can generalize the approach:

1. For each pair of images (Q_i, Q_j) , we can detect the common line angles θ_i and θ_j and write the equation:

$$\delta x_i \cos \theta_i + \delta y_i \sin \theta_i = \delta x_j \cos \theta_j + \delta y_j \sin \theta_j$$

2. This gives $\binom{N}{2}$ equations (one for each pair).
3. The unknowns are $\{(\delta x_i, \delta y_i)\}_{i=1}^N$, totaling $2N$ unknowns.
4. Typically, the shifts are constrained to have zero mean (or some other constraint), providing 2 additional equations:

$$\sum_{i=1}^N \delta x_i = 0, \quad \sum_{i=1}^N \delta y_i = 0$$

Number of Knowns and Unknowns

- **Unknowns:** $2N$ (all $\delta x_i, \delta y_i$).
- **Equations:**
 - From common lines: $\binom{N}{2} = \frac{N(N-1)}{2}$ (one per image pair).
 - Additional constraints: 2 (zero mean shifts).
 - Thus, the number of **Knowns** come out to be $\frac{N(N-1)}{2} + 2$
- For $N \geq 3$, the number of equations grows quadratically, while unknowns grow linearly, so the system is usually overdetermined and can be solved via least squares.

Solving the System

The system can be solved as follows:

1. Collect all pairwise common line equations.
2. Combine with zero-mean constraints.
3. Solve the resulting linear system $A\delta = \mathbf{b}$ for $\delta = (\delta x_1, \delta y_1, \dots, \delta x_N, \delta y_N)^T$ using least squares.

This approach allows the determination of the unknown 2D shifts in all projection images using common line constraints.